ELSEVIER

Polymer 43 (2002) 937–945

polymer

www.elsevier.com/locate/polymer

Effects of compatibilizing agent and in situ fibril on the morphology, interface and mechanical properties of EPDM/nylon copolymer blends

J. Ma[a,*], Y.X. Feng[b], J. Xu[a], M.L. Xiong[b], Y.J. Zhu[b], L.Q. Zhang[b,*]

[a]*State Key Laboratory of Polymer Physics and Chemistry, The Center for Molecular Science, Institute of Chemistry, The Chinese Academy of Sciences, Beijing 100080, People's Republic of China*

[b]*School of Materials Science and Engineering, Beijing University of Chemical Technology, Beijing 100029, People's Republic of China*

Received 26 February 2001; received in revised form 4 July 2001; accepted 26 August 2001

Abstract

The effect of several compatibilizers on mechanical property and morphology of ethylene–propylene diene monomer rubber (EPDM)/nylon copolymer (PA) blends was investigated. A significant reduction of dispersed phase dimension was observed when chlorinated polyethylene (CPE) was added to EPDM/PA blend, due to interaction that exists between CPE and PA. Based on differential thermal analysis, dynamic mechanical thermal analysis, scanning electron microscopy and transmission electron microscopy characterization, a speculative description of configuration was proposed to interpret the morphological investigation made on these blends. Cold milling of molten EPDM/PA/CPE blend gives rise to in situ fibril rubber compound, which can be mixed with curatives and statically vulcanized to give reinforced rubber compositions. Compared with vulcanized conventional rubber short fiber composites, the compositions show notably different elongation properties. The reason was given. It was shown that mechanical property of EPDM/PA/CPE blend could be improved by adding only a small amount of PA fibrils (i.e. 10%), which is different to that of conventional rubber short fiber composite. Based on above analysis, three forms of structures were proposed to discuss the relationship between the morphologies and mechanical properties. The studies of mechanical properties show that the materials obtained possess useful strength and excellent heat resistance. © 2001 Published by Elsevier Science Ltd.

Keywords: Ethylene–propylene diene monomer rubber/copolymerized nylon blends; Compatibilization; In situ

1. Introduction

This paper relates to an improved rubber compound, and more specifically relates to the improvement of the elastomeric components for tread pads of tracked vehicles, especially some endless track vehicles and other commercial type tracked vehicles. These tracked vehicles are frequently equipped with rubber track pads, rubber blocks or endless-band rubber track to reduce shock, noise, wear and damage to road surfaces. The vehicles travel over roads and hard surfaces and therefore the elastomeric components of the endless tracks should be of the type that wears well under abrasive rough terrain conditions. Track pads for shoes presently are often made by two routines. The first is that pads are made from special rubbers, such as highly saturated nitrile rubber (HNBR). The second is from common rubbers, such as styrene–butadiene rubber (SBR), natural rubber (NR), ethylene–propylene diene monomer rubber (EPDM), etc. The second gets more attention and the reason for it appears to be based on cost and the fact that at times it is required that the materials used in their devices be available from home sources to insure a continued supply.

Historically, field performance of these elastomeric track pad components has been poor, especially for the medium to heavy tonnage tracked vehicles, 40–60 tons. It required frequent and costly replacement of the elastomeric components. To improve field or service performance of pads, one must first identify those properties that are most needed and then optimize these. The elastomeric components of an endless track are affected in several ways depending upon service. Directly, it can cause cuts, tears, chunking, blow-outs and abrasive wear. Indirectly, it causes damage through hysteretic heating, environment convection and surface/terrain heating. Elastomer properties are often scaled by many parameters, such as hardness, elongation at break, tensile retention, tear strength, hot tear strength and heat-resistance, in which hot tear strength and heat-resistance are thought to be most dominant factors influencing the field

* Corresponding author. Tel.: +86-10-6443460; fax: +86-1-64434964.
E-mail address: genghp@buct.edu.cn (L.Q. Zhang).

0032-3861/02/$ - see front matter © 2001 Published by Elsevier Science Ltd.
PII: S0032-3861(01)00626-7

performance [1]. NR has excellent hot tear (at least 30 kN/m^{-1} at 121°C), but its heat-resistance is poor. For SBR, both hot tear and heat-resistance are poor. EPDM is well known for excellent heat-resistance attributed to its saturated backbone structure and nonpolarity. However, its tear strength, especially hot tear strength, is poor [2]. Ternary-nylon-copolymer with excellent strength and heat-resistance was copolymerized from nylon 6, nylon 66 and nylon 1010 by the ratio of 20/10/70. Rubber/plastic blends have been commercialized as rubber toughened plastics or as thermoplastic elastomers (TPEs) [3,4]. However, less attention was paid to rubber reinforced by plastics. In this study, we report on novel compositions of EPDM and PA compatibilized by chlorinated polyethylene (CPE), wherein the novel composition is characterized by in situ fibrils and highly improved tear and tensile strength at high temperature and excellent thermomechanical stability; wherein the improved composition is a unique combination of its respective polymer, filler and curing systems; whose composition is further well suited for manufacture of various abutment and motion stop or limit members subjectable to repetitive engagement by moving mechanisms.

2. Experimental

2.1. Materials

EPDM (ESPRENE501A, ESPRENE502) were purchased from the Sumitomo Chemical Corporation of Japan. PA150 (copolymerized from nylon 6, nylon 66 and nylon 1010 by the ratio of 20/10/70) and PA170 (copolymerized from nylon 6, nylon 66 and nylon 1010 by the ratio of 10/20/70) were provided by Sailulu Plastics Company of Shanghai. (CPE, content of chlorine, 35–37%) and carbon black (N220) were produced by Weifang Chemical Materials Company of Shangdong Province and Haitun Carbon Black Company of Tianjin, respectively. PA was dried at 60° for 12 h before use. Maleic anhydride-grafted EPDM (EPDM-*g*-MAH) and glycidyl methacrylate-grafted EPDM (EPDM-*g*-GMA) were made respectively according to literatures [5,6].

2.2. Processing

Compositions were prepared by a method named as two-step mixing. After PA was melted, CPE was added with the mixing. The mixing was continued until a fine dispersion occurred. The composition was then removed from the miller, and while still molten, passed once through a cold roll mill to give a sheet about 2 mm thick. The sheet was then cut into small pieces, which were remelted and mixed with EPDM until a fine dispersion occurred. Again, the mass was removed from the miller and while still molten, passed once through a tight cold roll mill to give rubber containing in situ-formed PA fibrils. Carbon black and curatives were incorporated into the composition, which was then statically cured (in a mold) at a temperature below PA melting point. The detailed procedure was reported in a previous article [7]. By this way, in situ fibril rubber compound was obtained. The processing of an incompatible thermotropic liquid crystalline polymer/thermoplastics (TLCP/TP) blend under an elongation at flow condition is known to produce an oriented TLCP-fiber phase [8–10]. Hence, the term 'in situ composite' was coined [11] for this type of polyblend, which means self-reinforcement due to the fibers formed during processing. The morphology in this study is similar to that mentioned above and hence, we use 'in situ fibril rubber composite' to describe this kind of blend.

2.3. Characterization

2.3.1. Mechanical testing

Specimen were die cut from the vulcanized sheet and used after at least 24 h storage at room temperature. The mechanical properties of the compositions were determined with test specimens at a constant temperature and humidity depicted by ISO test method [12].

2.3.2. Scanning electron microscopy

For SEM characterization plane surfaces were prepared on each specimen using a diamond knife at room temperature. To dissolve the dispersed phase, the specimens were allowed to stay in xylene at 20°C for 4 h. To avoid distortion of the polymer surface, a coating temperature of 40°C was chosen by moderating number and time of coating under a low electric current and a high voltage. Micrographs were obtained at magnifications ranging from 1000 to 10,000 using S-2501 SEM.

2.3.3. Transmission electron microscopy

TEM experiments were performed using a H-800 transmission electron microscope, in order to acquire a direct visualization of the particular morphological characteristics of the blends. Ultrathin sections of bulk samples of the blends were produced at −100°C using a Leica Ultracut UCT with EMFCS cryo-attachment. The sections were floated off the diamond knife and transferred to the grids. The specimens were stained with ruthenium tetroxide (R_uO_4) to enhance contrast between the phases [13].

2.3.4. Thermal analysis

A Perkin–Elmer DSC-3 was used to study the thermal behavior and microstructure. Measurements were made on approximately the same materials, which were cut from torn specimen. Glass transition temperatures, T_g, were obtained by heating and then cooling the sample over a temperature range of −80 to +100°C at 20°C/min.

Dynamic mechanical thermal analysis (DMTA) of the blends were performed on a DMTA Rheometric Scientific DDV-II-EA model. The experiments were carried out at a frequency of 11 Hz, a heating rate of 3°C/min and a double strain amplitude of 0.25% over a temperature range of −100

Table 1
Mechanical properties for EPDM/PA blends (EPDM 70 phr, PA 30 phr, Compatibilizer 15 phr, Stearic acid 1 phr, ZnO 5 phr, DCP 4 phr, Sulfur 1 phr, HVA-2 1 phr)

Blends	1	2	3	4	5
Compatibilizer	Nothing	EPDM-*g*-MAH	EPDM-*g*-GMA	CPE	IIR
Hardness (Shore A)	58	58	64	60	57
Tensile strength (MPa)	2.6	4.6	4.0	7.3	2.5
Elongation at break (%)	146	248	236	340	160
Tear strength (kN/m 25°C)	20.8	23.9	21.8	34.6	26.8

to +120°C. The loss tangent (tan δ) was measured for each sample in this temperature range.

3. Results and discussion

3.1. The effect of compatibilizers on blend property and morphology

It is well known that EPDM and PA are immiscible because their interfacial adhesion is weak; this results in their poor dispersion. To search for suitable compatibilizer, a series of polymers were investigated. As a reference, EPDM/PA blend was prepared by melt-mixing PA and EPDM on a rubber mill at 160°C for 8 min. Several compatibilizers, such as EPDM-*g*-MAH, EPDM-*g*-GMA and CPE, were chose to be melt-mixed with EPDM and PA on a rubber mill at 160°C for 8 min. It should be noted that the blends mentioned above were made by one-step mixing. EPDM/PA/butyl rubber (IIR) was prepared by two-step mixing shown in Section 2.

As seen in Table 1, blends compatibilized by EPDM-*g*-MAH or EPDM-*g*-GMA shows improved mechanical properties. However, the EPDM/PA/CPE blend shows the best properties. EPDM-*g*-MAH and EPDM-*g*-GMA were used as functional groups to produce chemical reaction with PA which was used as a meltable 'filler'. On the other hand, the backbone of grafted EPDM is compatible with the matrix polymer. As for EPDM/PA/CPE blend, the compatibilization is considered to occur through chemical bonds between CPE and PA molecules [14]. Previous work has confirmed the formation of a graft copolymer through reaction of aminolysis of the halogenated polymer by a terminal amine group of PA [14,15].

The difference in the microstructures of EPDM/PA, EPDM/PA/CPE and EPDM/PA/IIR was observed from cut and etched surfaces. Samples were prepared for SEM characterization according to Section 2. Fig. 1(a) is the surface of an EPDM/PA binary blend which will be used as a reference. It is seen that dispersed particles were etched by xylene and appear as dark fibrils with a length of about 30 μm on the cut surface. Fig. 1(b) is the surface of an EPDM/PA/CPE ternary blend. It shows the addition of CPE to the EPDM/PA blend resulted in much shorter fibril length. Fig. 1(c) is the surface of an EPDM/PA/IIR ternary

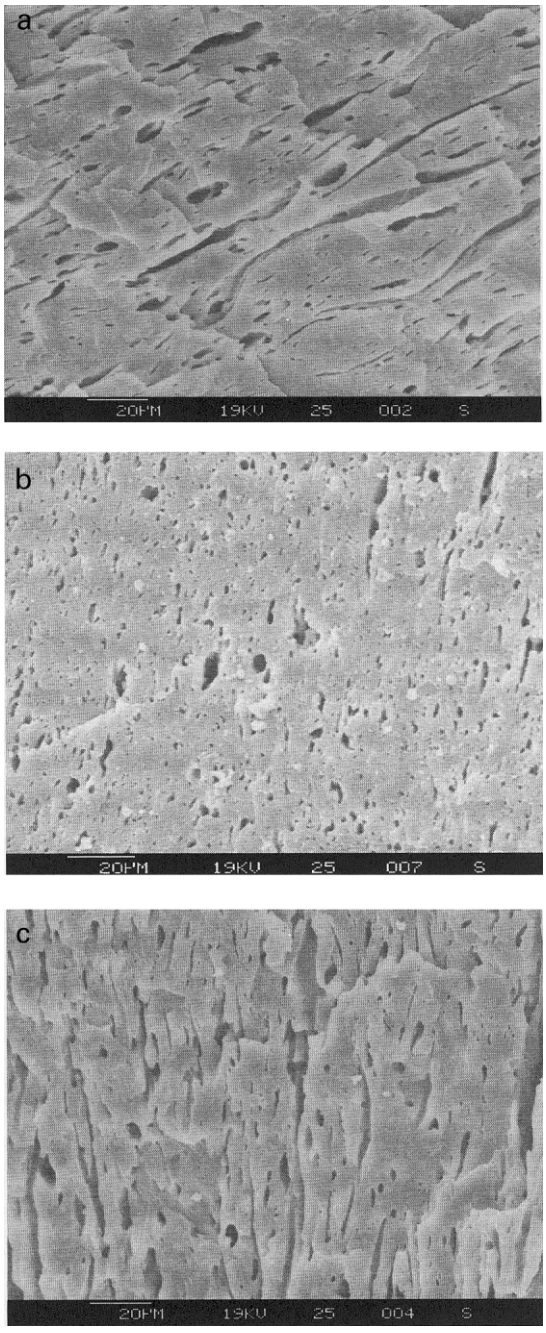

Fig. 1. SEM micrographs of cut surfaces of the EPDM/PA blends ((a)EPDM/PA; (b) EPDM/PA/CPE; (c) EPDM/PA/IIR).

Table 2
DSC data for components of EPDM/PA/CPE

Sample	EPDM	PA	CPE	PA	CPE	EPDM	PA	CPE
Structure	Separation	Separation	Separation	Blend of PA/CPE	Blend of PA/CPE	Blend of EPDM/PA/CPE	Blend of EPDM/PA/CPE	Blend of EPDM/PA/CPE
T_g (°C)	−52.2	93.8	−1.2	74.8	19.6	−52.2	70.8	12.6

blend in which, to our surprise, medium short fibril length was also observed. Butyl rubber (IIR) is nonpolar and cannot be used as a compatibilizer for EPDM/PA blend. Therefore longer short fibril should be observed, which conflicts with what is shown in Fig. 1(c). The experimental results thus can be interpreted by assuming that as in the first step IIR is anchored or inserted to PA, the viscosity of PA component become closer to matrix rubber and hence, resulted in the finer dispersion morphology in the second step. However, finer morphology does not always mean improved mechanical property. As shown in Table 1, the mechanical property of EPDM/PA/IIR is much lower than that of EPDM/PA/CPE. It is known that the morphology of a blend is determined by many parameters, such as the relative concentrations of each of the polymeric components, the viscosity ratio, the elasticity ratio of the individual polymeric components, the interfacial tension between the two polymeric components, the processing conditions, etc. [16–18]. In EPDM/PA/CPE blend, we found that the particle dimension of polymer blends strongly depends on the processing conditions than other parameters.

When CPE was used as a compatibilizer in EPDM/PA blend, the finest dispersed phase and the best mechanical properties were obtained. Theoretically, there are three possible arrangements in morphology of the blend. The first is that CPE and EPDM are mixed together to form bulk phase. The second is that CPE and PA are mixed together to form disperse particles. The last is that CPE molecules locate at the interfaces between EPDM bulk and PA dispersed particles. Further characterization shows that the second speculation is the most probable one.

3.2. Thermal analyses

DSC has shown the improvement of compatibility between EPDM and PA after addition of CPE in the EPDM/PA blend. Compatibility between polymers can be characterized by their glass transition temperature difference, ΔT_g. Tables 2 and 3 give the effect of the added component on the T_g of EPDM and PA. In Table 3, it is seen that the ΔT_g of PA and CPE is 95.0°C, and while PA and CPE melt were blended, ΔT_g of them decreased to 55.2°C. It can be explained by chemical reaction between PA and CPE phase. In EPDM/PA/CPE blend, as shown in Table 2, addition of CPE significantly decreased the T_g of PA, but did not affect the T_g of EPDM. T_g of CPE also increased because of its reactivity to PA. As shown in Table 3, the ΔT_g of EPDM and PA is decreased by 15.8% with the addition of CPE. The compatibility of EPDM and PA was clearly improved, which corresponds with the SEM observation.

Fig. 2 represents the DMTA results of EPDM/PA blend (70/30) and EPDM/PA/CPE blend (70/30/15) in terms of temperature dependence of tan δ in the temperature range between −100 and 120°C. All blends show two damping peaks, one at −45°C corresponding to the glass–rubber

Table 3
DSC data for components of EPDM/PA/CPE

Sample	PA/CPE	PA/CPE	EPDM/PA	EPDM/PA
Structure	Separation	Blend of PA/CPE	Separation	Blend of EPDM/PA/CPE
ΔT_g (°C)	95.0	55.2	146.0	123.0

transition of EPDM, the other peak at 30–40°C due to T_g of PA. The latter peak is found to be very broad. It is because of the diversified block backbone structure of PA, which is copolymerized from different-reactive monomers, (i.e. nylon 6, nylon 66 and nylon 1010, by the ratio of 20/10/70). Orientation of dispersed particle in blending process also promotes the broadening of the peak.

Though the peak position of PA of EPDM/PA/CPE is shifted compared to that of EPDM/PA blend due to interaction between the blend components, the appearance of two separate tan δ strongly suggests the microheterogeneity of the blend (i.e. two phase morphological structure) and hence, the incompatibility of the blend components. This is further revealed from the scanning electron micrographs (Fig. 1). However, addition of CPE significantly decreased the T_g of PA, but did not affect the T_g of EPDM.

The above result, i.e. the change of the tan δ with the addition of CPE, can be discussed in the light of structural changes associated with the interaction between PA and CPE phases. It is known that the height of the dynamic transition of a component of a composite apparently reflects the relative quantity of the component itself [18–20]. Also, the model calculation based on the modified Kerner equation and presented in detail by Dickei [21] indicates that the height of the dispersed phase loss peak is principally a function of inclusion volume fraction. Thus, it may be said that the increase of tan δ of PA in the blend is the result of reduction of the relative quantity of bulk rubber in the blends. Since the weight fraction of PA in this blend is constant, such an increase may be interpreted as the progressive mobilization of the CPE chains into the dispersed particle when they are grafted to the PA. The experimental results thus can be interpreted by assuming that as CPE is anchored to the dispersed phase, the relative volume of the PA increases resulting in the reduction of the relative quantity of the bulk rubber and hence, results in the reduction of the tan δ values. The broadening of the tan δ peak of PA is found to occur with the addition of CPE and the reason for it is that the grafting of CPE to PA made the component of PA more diversified.

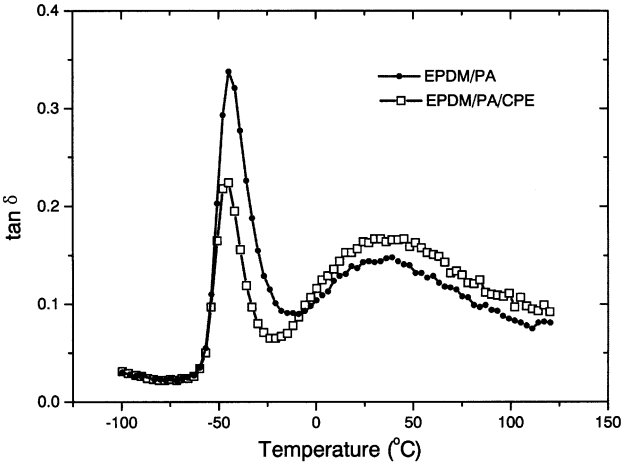

Fig. 2. DMTA results for the compatibilized and uncompatibilized EPDM/PA blends.

The second result, i.e. the decrease in T_g of PA suggests that the segmental motion of the PA chains occurs at lower temperatures in the ternary blend than in EPDM/PA blend. It is reported [22] that the segmental motion in chains of a polymer when attached to a more mobile component (i.e. lower T_g) is enhanced in the blend compared to that in the homopolymer. As PA chains are grafted to a more soft component having a lower T_g, the molecular flexibility of the PA chains is expected to be increased leading to a decrease in its T_g values.

Based on DSC and DMA analysis, a conclusion could be drawn that EPDM is the matrix polymer and CPE is mainly blended into dispersed particle. The addition of CPE makes dispersed particle smaller and well distributed and thus significantly increases interaction between the two phases. The result is sustained by TEM observation. Fig. 3 shows the ultrathin surfaces cut by a microtome below −100°C and stained with ruthenium tetroxide (RuO_4). It is seen that CPE molecules are anchored or inserted into dispersed particles because of the chemical reaction between PA and CPE.

3.3. In situ fibril rubber compound

It is well known that rubber is generally reinforced by carbon black (i.e. recipe 1 in Table 4). In this study, 15 phr of carbon black were replaced by PA and after the cold milling of molten EPDM/PA/CPE blend, in situ fibril rubber composite was obtained. Coran and Patel [23] first reported the cold milling of melt-mixed composition of CPE/nylon results in nylon-reinforced rubber which can be mixed with curatives and statically vulcanized below the melting temperature of the nylon to give reinforced rubber compositions which resemble the case of vulcanized rubber-short fiber composition [24,25]. However, microstructure analysis and elongation value were unavailable from those papers.

As shown in Table 4, replacement of carbon black by PA renders the rubber higher strength, especially hot tear

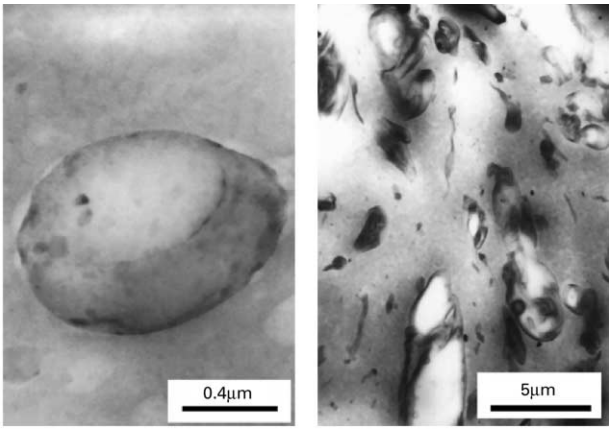

Fig. 3. TEM micrographs of the EPDM/PA blends.

strength, and lower dynamic heat build-up while the blend holding the similar hardness and heat-resistance.

Fibrillous morphology can be clearly observed from surfaces cut along three planes.

X-plane: cut along one plane that is vertical to grain direction. As shown in Fig. 4(a), dispersed fibrils were etched by xylene and appear as two kinds of shapes: short fiber-like and dot-like holes.

Y-plane: cut along one plane that is parallel to grain direction and vertical to grain plane. As shown in Fig. 4(b), dispersed fibrils show similar above-mentioned shapes.

Z-plane: cut along one plane that is parallel to grain plane. As shown in Fig. 4(c), dispersed fibrils were etched by xylene and appeared as three kinds of shapes: plate-like, short fiber-like and dot-like holes. All above images show fibrillous morphology. Dot-like holes could be morphology of cross-section of fibrils. In situ fibril rubber composite was obtained after the cold milling of melt-mixed EPDM/PA/CPE and then the following processing made these fibrils oriented disorderly. Finally, the fibrils oriented disorderly in one plane vertical to vulcanization's tension during vulcanization in which some fibrils melted again and formed plate-like morphology.

Table 4
Mechanical properties of EPDM and EPDM/PA/CPE

Recipe	1[a]	2[b]
Tensile strength (MPa)	13.1	17.5
Hardness (SH A)	81	80
Elongation at break (%)	380	360
Tear strength (kN/m 25°C)	38.5	57.2
Tear strength (kN/m 121°C)	8.6	17.2
Internal temperature rise/°C	106	80
Surface temperature rise/°C	30	24
After oven aging 70 h at 121°C, elongation retention (%)	72	63
After oven aging 70 h at 121°C, tensile retention (%)	100	100

[a] Recipe 1 EPDM 70 phr, Stearic acid 1 phr, ZnO 5 phr, Carbon Black 35 phr, DCP 4 phr, Sulfur 1 phr, HVA-2 1 phr.

[b] Recipe 2 EPDM 70 phr, PA 30 phr, CPE 15 phr, Stearic acid 1 phr, ZnO 5 phr, Carbon Black 35 phr, DCP 4 phr, Sulfur 1 phr, HVA-2 1 phr.

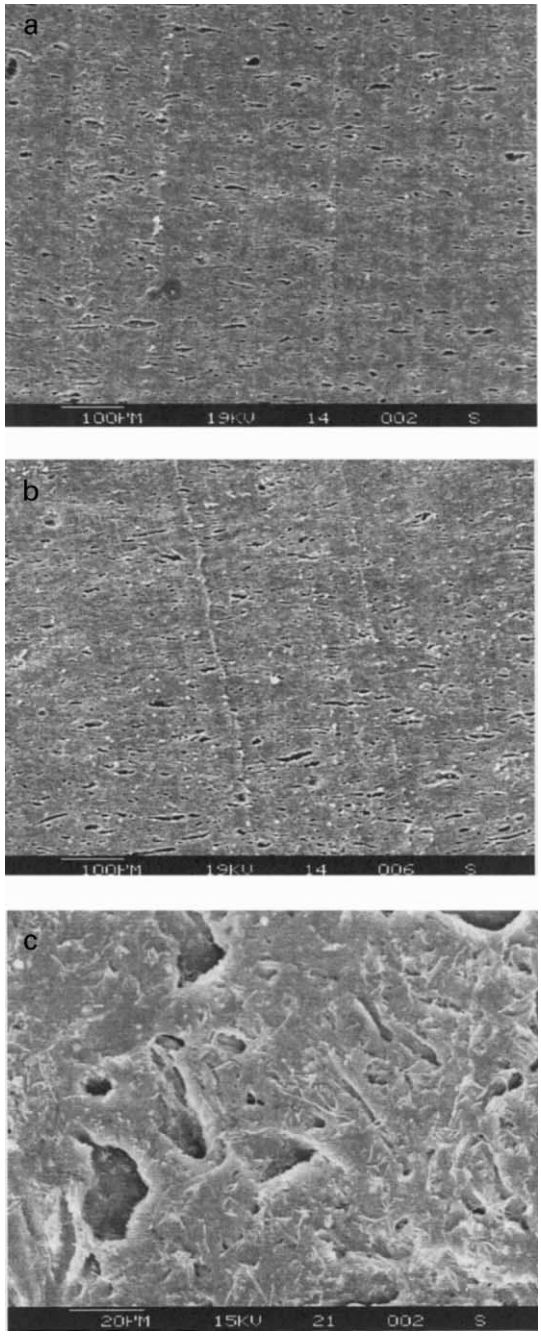

Fig. 4. SEM micrographs of cut and etched surfaces of the EDPM/PA blends cut along different directions ((a) along *X*-directions; (b) along *Y*-direction; (c) along *Z*-direction.

By processing control, in situ fibril rubber composite was obtained which showed remarkable properties. Tensile strength and elongation at break along longitudinal direction (LD) and transverse direction (TD) and their ratios (δ_L/δ_T and $\varepsilon_L/\varepsilon_T$) are listed in Table 5.

The clear difference in tensile strength and elongation along two vertical direction suggests that the cold milling

Table 5
Mechanical properties of in situ fibril rubber composite along different directions of fibril

EPDM/PA/CPE	*L*-direction	*T*-direction	*L/T*
Tensile strengh (MPa)	22.3	13.8	1.62
Elongation ratio at break (%)	368	244	1.51

produced dispersed particles of fibrillous morphology. It is surprisingly found that $\varepsilon_L/\varepsilon_T > 1$ occurs in this in situ fibril rubber composite. In conventional rubber-short fiber composites, however, the ratio is always smaller than 1. This contrasting feature could be explained in the light of the size and the property of dispersed phase.

Firstly, dimensions of dispersed phases are wholly different. In in situ fibril rubber composite, stick-like dispersed particle with a diameter of 1–3 μm and a length of 10–50 μm is easy to stiffen or constrain the matrix rubber to permit effective load transfer across the hard–soft interface without fiber rupture while stretched along LD. While stretched along TD, it seems that in situ fibril becomes deleterious for the reason of uneven of load on fibril and hence, smaller elongation was observed. In rubber-short fiber composites, however, dispersed particle with a diameter of 3–50 μm and a length of more than 3000 μm is easy to correspond to load while stretched along TD just because of its great length. While stretched along LD, the long fiber could not constrain the matrix rubber to efficiently carry away load or stress across the hard–soft interface without fiber rupture because of the excessive length and hence, got lower elongation.

Secondly, in in situ fibril rubber composite, rubber was reinforced by PA, which is copolymerized from nylon 6, nylon 66 and nylon 1010 by the ratio of 20/10/70 and has the elongation of 1000%. After CPE is added in EPDM/PA, the elongation of dispersed phase is believed to increase significantly. While stretched along LD, it is easier to transfer load from bulk rubber. While stretched along TD, it is more difficult to do it for the reason of its short length. In rubber-short fiber composites, rubber was reinforced by nylon (i.e. nylon 6), which has the elongation of less than 100%. While stretched along TD, the long fiber is easy to correspond to the stress and load. While stretched along LD, the poor elongation of PA and poor compatibility between rubber and nylon seem to limit its corresponding to stress and load.

Compared with short-fiber rubber composite, in situ fibril rubber compound shows lower hardness, lower heat build-up, smaller dispersed phase, larger elongation, lower erasion and convenience to be processed. In short-fiber rubber composite, it was believed that lower concentrations (i.e. 10%) of fiber are deleterious because they need enough fibers to stiffen or constrain the matrix rubber to permit effective load transfer across the hard–soft interface without fiber rupture. For in situ fibril rubber compound, however, mechanical properties could be improved with addition of a small amount of PA. As shown in Fig. 5, tensile strength, tear strength and elongation were notably improved with addition of 10% PA to bulk rubber. It could be explained as in in situ fibril rubber composite the polarity-matched rubber/plastic blend, the finer dispersed particles and long elongation of PA make dispersed particles easier to correspond to stiffen or constrain the matrix rubber to permit effective load transfer across the hard–soft interface than those in rubber short fiber composite.

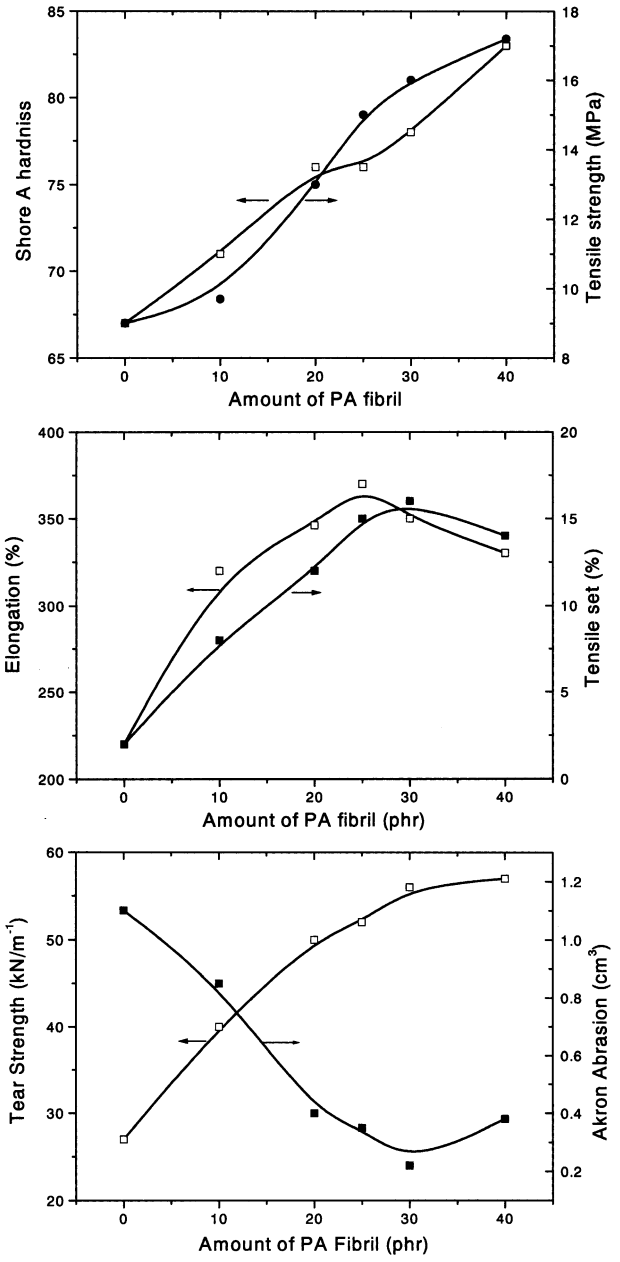

Fig. 5. Mechanical properties of in situ rubber composite with different amount PA fibril.

3.4. Relationships between structure and property

It is well known that polymer property will always be

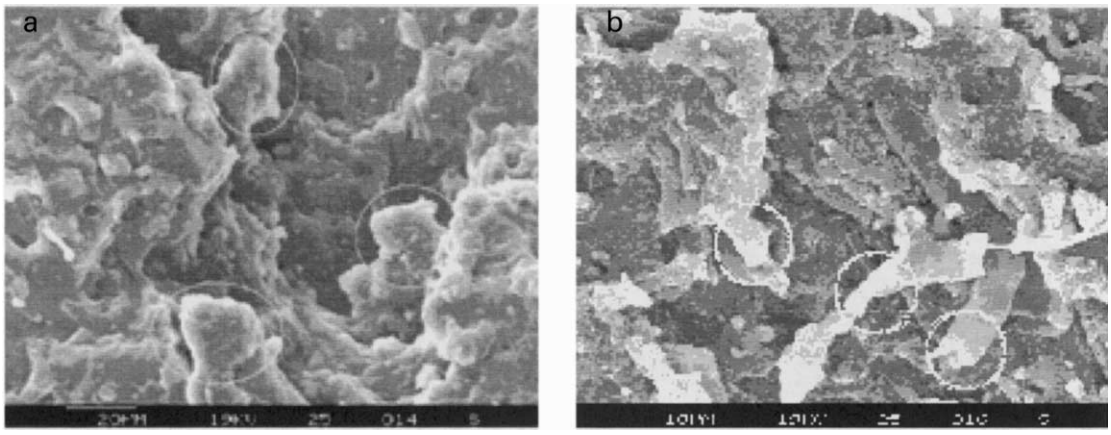

Fig. 6. SEM micrographs of EPDM/PA/CPE (70/30/15) blends broken in various environments. (a) Broken surfaces given by pulling specimen. (b) Broken surfaces given by wearing and tearing specimen.

determined by its corresponding structure. To understand relationship between structure and property of EPDM/PA/CPE blend, three forms of structure were proposed according to different morphological dimensions shown in TEM and SEM observation.

The inserted structure refers to CPE inserting or anchoring into PA forms dispersed particles with dimension of 2 μm or so. The anchored or inserted structure reduces the polarity of PA and makes its viscosity closer to the bulk polymer and therefore, compatibility between EPDM and PA would be improved significantly which could be apparent in SEM, DSC and DMA characterization. The structure is responsible for the blend to combine excellent mechanical properties of PA with good heat resistance of EPDM.

The in situ fibril structure refers to in situ fibrils with diameter of 1–3 μm and length of 10–50 μm. Self-reinforcement was realized due to the fibrils formed through tightly cold milling of melt-mixed EPDM/PA/CPE blend. Compared with irregularly dispersed particles, in situ fibril possesses higher surface area per unit volume and would be easier to stiffen or constrain the matrix polymer to permit effective stress transfer across the hard–soft interface. In comparison to conventional rubber short fiber composite, two notably different properties were found for the in situ fibril structure. One is that mechanical property of EPDM could be significantly improved with less amount of PA fibril (i.e. 10%) shown in Fig. 5. The other is its surprisingly elongation ratio along TD and LD shown in Table 5.

The aggregated structure which must be considered in this study relating polymer structure to polymer properties is aggregation of domains with diameters of more than 3 μm composed of fibrils and bulk polymer. Only under external stress, aggregation could be formed and then greater stress or longer stress period might lead to breakage at the fringe of aggregation. That could be proved by analysis of SEM observation of 'small fibers' on the surfaces of broken specimen. As shown in Fig. 6(a), some 'small fibers' named as aggregation with a diameter of about 20 μm were observed. The length is larger than that of the fibril. When the composite was stretched, bulk rubber corresponds to constrain the load stress and breakage happened first at the fringe of aggregation. Under different strain and stress, aggregations could have different dimensions. As shown in Fig. 6(b), there are some aggregations with a smaller diameter of about 5 μm, which could be caused by small but sustaining abrasive force.

To obtain useful high performance rubber compound with

Table 6
Comparison of mechanical propoties of various recipes

Recipe	COV standard T-107[a]	M-60 standard T-142[a]	EPDM/PA/CPE[b](75/25/12)
Tensile strength (MPa)	21.2	19.8	20.6
Hardness (Shore A)	64	69	81
Elongation at break (%)	520	510	380
Tear strength (kN/m 25°C)	47.5	55.4	65.8
Tear strength (kN/m 121°C)	27.2	20.6	23.7
After oven aging 70 h at 121°C, elongation retention (%)	12	38	63
After oven aging 70 h at 121°C, tensile retention (%)	45	57	100

[a] From US patent 4,843,114.
[b] EPDM (ESPRENE502) 75 phr, PA170 25 phr, Compatibilizer 12 phr, Carbon Black 35 phr, Stearic acid 1 phr, ZnO 5 phr, DCP 4 phr, Sulfur 1 phr, HVA-2 1 phr.

low cost, extensive studies were performed [26,27]. As shown in Table 6, the best result is compared with the data from US Patent 4,843,114 in which the track pads designated STD. T-107 and STD. T-142 were standard stock pads for the American Army's experimental counter obstacle vehicle (COV), and the M-60 tank respectively, made from SBR.

4. Conclusions

CPE was found to be an efficient compatibilizer for EPDM/PA blend. Addition of CPE significantly decreased the T_g of PA, but did not affect the T_g of EPDM. CPE was anchored into dispersed PA particles and therefore the relative volume of the PA increased resulting in the reduction of the relative quantity of the bulk rubber that caused the reduction of the tan δ values.

From SEM micrographs of cut surfaces, the cold milling of molten EPDM/PA/CPE blend was found to cause the formation of in situ fibril rubber compound, which displayed a magnificently improved tear strength. It was of interest that $\varepsilon_L/\varepsilon_T > 1$ occurs in this in situ fibril rubber composite which is different to that of conventional rubber short fiber composite. It was surprisingly found that small amount of PA fibril (i.e. 10%) actually reinforced the mechanical properties of the matrix rubber. In rubber short fiber composite, however, such low concentrations of fiber are deleterious for the properties of the matrix rubber. It can be explained that, in in situ fibril rubber composite, the polarity-matched rubber/plastic blend, the finer dispersed particles and long elongation of PA make dispersed particles easier to correspond to stiffen or constrain the matrix rubber to permit effective load transfer across the hard–soft interface than those in rubber short fiber composite.

The relationship between the morphologies and mechanical properties was discussed in the light of three forms of structures proposed according to different morphological dimensions observed in TEM and SEM observation.

EPDM/PA/CPE blends shows highly improved mechanical properties, especially hot tear strength, and excellent heat resistance with low cost. These systems offer promise for manufacture of tread pads of various tracked vehicles.

Acknowledgements

The authors thank the Ministry of Chemical Technology of China for a grant. J. Ma thanks Prof. L.H. Shi for providing the useful instructions and Y.X. Shi for helping to carry out the experiments.

References

[1] Zhang LQ, Geng HP, Chen S. China Synth Rubber Ind 1996;19:325–30.
[2] Ma J, Zhu YJ. China Synth Rubber Ind 2000;23:186–91.
[3] Bucknall CB. Toughened plastics. London: Applied Science Publishers, 1977. Chapter 2.
[4] Coran AY. Thermoplastic elastomers. New York: Hanser Publishers, 1987. Chapter 3.
[5] Darilyn H. Polym Engng Sci 1997;37:1421–6.
[6] Moffett AJ, Dekkers ME. Polym Engng Sci 1992;32:1–5.
[7] Ma J, Zhu YJ. China Rubber Ind 2000;47:323–30.
[8] Dutta D, Fruitwala H, Kohli A, Weiss RA. Polym Engng Sci 1990;30:1005–18.
[9] Handlos DG, Baird JM. Rev Macromol Chem Phys C 1995;35:183.
[10] Acierno AA. Rheology and processing of liquid crystalline polymers. London: Chapman & Hall, 1996.
[11] Kiss G. Polym Engng Sci 1987;27:410–23.
[12] Liu ZR, Tang HY. Experimental procedure. Handbook of Rubber Industry, No. 8. Beijing: Chemical Technology Press. p. 557–91.
[13] Trent JS, Scheinbeim JI, Couchman PR. Macromolecules 1983;16:589–98.
[14] Ma J, Zhu YJ. China Synth Rubber Ind 1999;22:358–61.
[15] Coran AY, Patel R. Rubber Chem Technol 1983;56:210–25.
[16] Coran AY. Rubber Chem Technol 1997;70:781–97.
[17] Willis JM, Caldas V, Favis BD. J Mater Sci 1991;26:4742–50.
[18] Mccrum NG. J Polym Sci 1958;27:555–97.
[19] Mccrum NG. J Polym Sci 1959;34:355–69.
[20] Mccrum NG. Makromol Chem 1959;34:50.
[21] Dickie RA. Polymer blends, vol. 1. New York: Academic Press, 1978.
[22] Eastmond GC, Smith EG. Polymer 1977;18:244–50.
[23] Coran AY, Patel R. Rubber Chem Technol 1983;56:210–25.
[24] Boustany K, Coran AY. US 3, 697, 364 (October 19, 1972).
[25] Boustany K, Coran AY. Rubber Chem Technol 1974;47:363–75.
[26] Ma J, Zhu YJ. China Rubber Ind 2000;47:588–93.
[27] Ma J, Zhu YJ. China Polym Mater Sci Engng 2001;17(3):126–30.